

# Material contrast does not predict earthquake rupture propagation direction

Ruth A. Harris

U.S. Geological Survey, Menlo Park, California, USA

Steven M. Day

Department of Geological Sciences, San Diego State University, San Diego, California, USA

Received 30 June 2005; revised 3 October 2005; accepted 10 October 2005; published 1 December 2005.

[1] Earthquakes often occur on faults that juxtapose different rocks. The result is rupture behavior that differs from that of an earthquake occurring on a fault in a homogeneous material. Previous 2D numerical simulations have studied simple cases of earthquake rupture propagation where there is a material contrast across a fault and have come to two different conclusions: 1) earthquake rupture propagation direction can be predicted from the material contrast, and 2) earthquake rupture propagation direction cannot be predicted from the material contrast. In this paper we provide observational evidence from 70 years of earthquakes at Parkfield, CA, and new 3D numerical simulations. Both the observations and the numerical simulations demonstrate that earthquake rupture propagation direction is unlikely to be predictable on the basis of a material contrast. **Citation:** Harris, R. A., and S. M. Day (2005), Material contrast does not predict earthquake rupture propagation direction, *Geophys. Res. Lett.*, 32, L23301, doi:10.1029/2005GL023941.

## 1. Introduction

[2] What allows large earthquakes to occur repeatedly on faults, without generating much heat? One mechanism proposed in the 1990's invoked a contrast in compliance (due to rock-type difference) across a fault, whereby an earthquake dynamically relieves normal stress on the fault on which it is propagating [Andrews and Ben-Zion, 1997]. Some numerical experiments have suggested that there would be a preferred direction of rupture as a consequence of these normal stress fluctuations. Since increased ground motion [Boatwright and Boore, 1982; Somerville et al., 1997] damage, and triggered seismicity [Gomberg et al., 2001] are often observed in the forward direction of a propagating earthquake rupture, predicting propagation direction would be a step towards deterministic hazard prediction. Here we show that earthquakes on the Parkfield section of the San Andreas fault do not support the hypothesis that rupture propagation direction is predictable from rock compliance contrast. A series of magnitude 4 to magnitude 6 Parkfield earthquakes from 1934 to 2004 did not all propagate in the direction predicted by their surrounding rock types. Nor do numerical simulations that include a reduction in friction coefficient during sliding [Harris and Day, 1997] predict a preferred rupture direc-

tion. Instead we propose that propagation direction at Parkfield and elsewhere is controlled by fault geometry and rheology.

## 2. Computer Simulations of Earthquakes: Preferred Direction Hypothesis

[3] To address the question of what determines rupture propagation direction, scientists have explored computer simulations of earthquakes. One set of computer simulations has examined earthquake behavior for the case of a fault that bounds two different rock types. These 2D simulations predict results that depend on the assumed friction formulation. One end-member case of these computer simulations assumes the friction coefficient to be constant, that is the static and kinetic coefficients of friction are equal. Stress variations, induced by contrast in rock type across the fault, then dominate the earthquake dynamics, and this end-member case generally predicts that the preferred propagation direction for earthquakes should be in the slip direction of the 'softer' (lower shear modulus) rock [Andrews and Ben-Zion, 1997; Ben-Zion and Andrews, 1998; Cochard and Rice, 2000; Ranjith and Rice, 2001]. As an example, if a right-lateral strike-slip fault strikes NW-SE and has softer rocks on the NE side of the fault, then this 'preferred-direction' hypothesis would have earthquakes on this fault rupturing from NW to SE (Figure 1a).

## 3. Computer Simulations of Earthquakes: No-Preferred Direction Hypothesis

[4] Concurrent work [Harris and Day, 1997] has examined a second end-member case of computer simulations in which the friction coefficient transitions between static and kinetic states when fault sliding begins. For this second end-member case, numerical simulations show that the frictional transition dominates over rock-type induced stress fluctuations: simulations with frictional-transition show rupture-velocity and slip-velocity asymmetries, and occasional supershear speeds, due to the stress fluctuations induced by the material contrasts. However the simulated earthquake rupture is bilateral. This alternate 'no-preferred-direction' hypothesis would have the earthquakes on the NW-SE striking fault rupturing both to the NW and to the SE (Figure 1b). Interestingly, lab experiments of crack behavior in the material homalite [Xia et al., 2005] agree with the Harris and Day [1997] numerical simulations. Similar to the numerical simulations, the lab experiments also do not

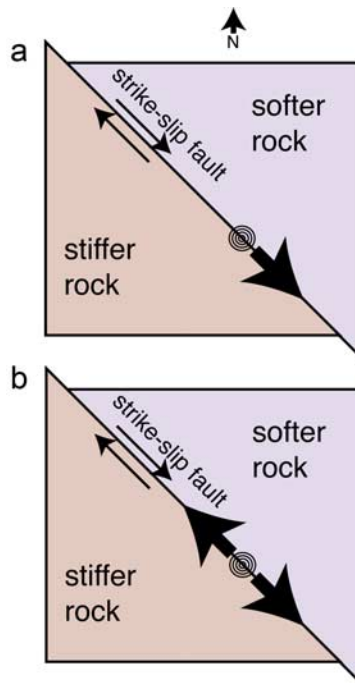


**Figure 1.** Schematic showing direction of rupture propagation for an earthquake that nucleates (circles) on a NW-SE striking, vertical right-lateral strike-slip fault that serves as the boundary between a ‘softer’ (lower value of  $((\text{density}) \times (\text{shear-wave})^2)$  rock and a ‘stiffer’ (higher value of  $((\text{density}) \times (\text{shear-wave})^2)$  rock. a) In the preferred-direction hypothesis the material contrast across the fault leads to rupture propagation in the slip-direction of the ‘softer’ rock. b) In the alternate hypothesis the material contrast leads to rupture propagation in both along-strike directions.

show a preferred propagation direction in the presence of a material contrast.

#### 4. Observational Evidence

[5] Although much can be learned from computer and lab simulations of earthquakes and cracks, the observations of actual earthquakes serve to test the computational- and lab-based hypotheses. For the material contrast case the observational evidence has been relatively sparse, with one exception. This exception is the San Andreas fault near Parkfield, California. The Parkfield site has been intensely monitored for more than 20 years due to its recurring M6 earthquakes, the most recent of which occurred in 2004 [Langbein *et al.*, 2005]. Observational data from Parkfield earthquakes extend to the 1800’s, but the best recorded events have occurred since the 1930’s. Next we show how Parkfield earthquakes from 1934 to 2004 and with magnitudes ranging from M4 to M6, disagree with the preferred-direction hypothesis (Figure 2).

[6] The San Andreas fault is a right-lateral strike-slip fault. Near Parkfield the fault mainly offsets Franciscan assemblage rocks on the NE side of the fault from Salinian granitic rocks on the SW side of the fault [Dibblee, 1971; Eberhart-Phillips and Michael, 1993], leading to predominantly ‘softer’ rocks on the NE side, and predominantly

‘stiffer’ rocks on the SW side. Using this simple model of material contrast across a fault, the preferred-direction hypothesis would have all Parkfield San Andreas earthquakes rupturing the fault from NW to SE (Figure 1a). Many earthquakes at Parkfield have shown this behavior. In 1934 an M6 Parkfield earthquake occurred and regional seismograms show that it nucleated in the NW and subsequently ruptured along the San Andreas fault to the SE [Bakun and McEvilly, 1979, 1984]. A similar event occurred in 1966 when the San Andreas fault once again slipped in an M6 Parkfield earthquake that ruptured from NW to SE [Bakun and McEvilly, 1979, 1984]. However neither the 1934 nor the 1966 M6 earthquakes were solo events. Instead both M6 earthquakes had M5 foreshocks, the closest event in time to each M6 being a 17-minute earlier M5 foreshock. In both 1934 and 1966 the M5 foreshocks nucleated in the same region as their subsequent M6 mainshocks, but rather than propagating from NW to SE, both of the M5 foreshocks propagated along the San Andreas fault from SE to NW [Bakun and McEvilly, 1979].

[7] Taken together, the M6 1934 and 1966 Parkfield mainshocks appear to endorse the preferred-direction hypothesis, since both earthquakes propagated in the predicted direction for this section of the San Andreas fault. However, the M5 foreshocks, whose rupture directions were opposite to their hypothesized pathways, conflict with the preferred-direction hypothesis. The evidence against the preferred-direction hypothesis mounts as one marches forward in time and examines other Parkfield earthquakes.

[8] In 1992, 1993, and 1994, magnitude 4 (M4+) earthquakes occurred in the area of the San Andreas fault where the 1966 M6 mainshock started. These moderate 1990’s earthquakes were shown to have propagated upwards and to

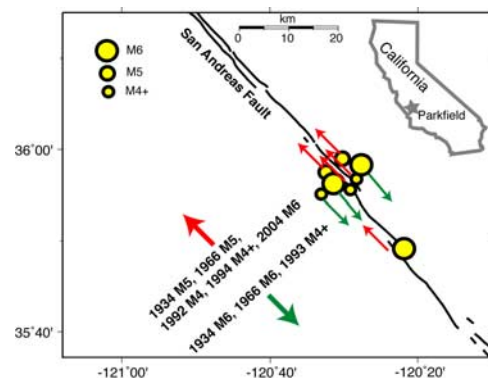


**Figure 2.** Well-studied earthquakes in the Parkfield, CA region of the San Andreas fault, and their propagation directions. M6 earthquakes in 1934, 1966, and 2004 ruptured the San Andreas from NW to SE, NW to SE, and SE to NW, respectively [Bakun and McEvilly, 1979; Langbein *et al.*, 2005]. M5 earthquakes in 1934 and 1966 both ruptured the San Andreas from SE to NW [Bakun and McEvilly, 1979]. M4+ earthquakes in 1992 (M4.3), 1993 (M4.6), and 1994 (M4.7) ruptured the San Andreas upwards to the SE (1993), and upwards to the NW (1992, 1994) [Fletcher and Spudich, 1998]. Earthquakes (circles) are shown at their approximate nucleation sites along strike of the fault, but to better show all of the events some have been moved outward, perpendicular to the San Andreas.

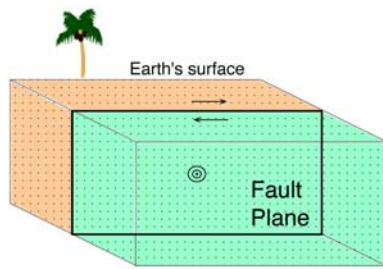


**Figure 3.** 3D computer simulations of an earthquake propagating on a right-lateral vertical-strike-slip fault. The rock on the far side of the fault is softer than the rock on the near side. The simulated earthquake is artificially nucleated in the middle of the fault at 0 seconds then spontaneously propagates. (a) Schematic showing the 3D finite-difference grid used for the simulations. The simulated earthquake nucleates at the circles. (b) Spontaneous rupture simulations. On the near side of the fault  $V_p = 6000$  m/s,  $V_s = 3464$  m/s. On the far side of the fault  $V_p = 5000$  m/s,  $V_s = 2887$  m/s. The density  $2670$  kg/m<sup>3</sup> is the same for both sides. Each frame shows a snapshot of the rupture at 0.5 second intervals. Contours show the differential horizontal slip-velocity (m/s). Note that the rupture propagates in both along-strike directions, to the right and, left. (c) Same as (b) except that on the far side of the fault  $V_p = 4000$  m/s,  $V_s = 2309$  m/s. Note that the rupture propagates in both along-strike directions, to the right and, left. To the left the propagation speed is supershear,  $>V_s$ , as observed in 2D simulations by *Harris and Day* [1997].

the SE (one earthquake), and upwards and to the NW (two earthquakes), rather than NW to SE [*Fletcher and Spudich*, 1998].

[9] In 2004 the most recent M6 Parkfield earthquake occurred, on the same portion of the fault as 1934 and 1966. A surprise for those anticipating the recent M6 earthquake was its propagation direction. Unlike its 1934 and 1966 M6 predecessors, the 2004 M6 earthquake propagated on the San Andreas fault primarily from SE to NW [*Fletcher and Spudich*, 2004; *Langbein et al.*, 2005].

[10] To summarize, two M6 Parkfield earthquakes have propagated in the direction that would be predicted by the preferred-direction hypothesis, and one M6, two M5 and two M4 earthquakes have propagated in directions not predicted by this hypothesis (Figures 1 and 2). Therefore the observational evidence seems to require another explanation for the propagation directions of earthquakes.

## 5. New 3D Computer Simulations of Earthquakes

[11] Before abandoning the computationally-based preferred-direction hypothesis, one more numerical test needs to be done. Since all of the aforementioned numerical studies were for the 2D case of a fault bounded by contrasting materials, here we also examine 3D simulations to test if including the third dimension might alter our hypotheses about rupture propagation direction. The third dimension is of large significance for the material contrast scenario because only in the 2D in-plane (along-strike, for a strike-slip fault) situation are the shear and normal stresses coupled. In 3D the anti-plane (along-dip for strike-slip)

contribution can also be significant, and the anti-plane solution behaves differently than the in-plane solution.

[12] For numerical comparison with earlier 2D simulations [*Harris and Day*, 1997], we use the same initial conditions and friction parameters, and the same methodology. The 3D numerical simulations use a 3D finite-difference computer program [*Day*, 1982; *Day and Ely*, 2002] and invoke artificial nucleation at the hypocenter followed by spontaneous (unforced) rupture propagation. The slip-weakening fracture criterion [*Ida*, 1972] allows the rupture to propagate as long as points on the fault plane meet or exceed the slip-dependent failure threshold. Since there is a material contrast across the fault, the normal stress does not remain constant, but instead varies. We take the frictional stress to be proportional to the normal stress. Because of the instantaneous response of frictional stress to normal stress change, the perfectly elastic problem is ill-posed, in the sense that steady sliding is unstable to perturbations of all wavelengths [*Adams*, 1995]. We regularize the problem by making the medium Kelvin-Voigt viscoelastic, which eliminates the exponential growth of short-wavelength perturbations and makes the problem analytically well-posed, as well as numerically well-behaved. The finite-difference simulations use a node-spacing of 50 m (similar results were produced using 25 m), a slip-weakening critical distance of 0.1 m, and static and kinetic friction coefficients of 0.6 and 0.5, respectively. The initial shear and normal stresses are 107.5 MPa and 200 MPa, respectively.

[13] Figure 3 shows the simulations for the cases of 17% and 33% contrast across a vertical right-lateral strike-slip fault with faster material on the ‘closer’ side of the fault, and slower material on the ‘farther’ side of the fault. Even though the full 3D solution incorporates many more features than are permitted in 2D, we find that the behavior in the along-strike direction is the same for the 3D and 2D cases. The 3D case shows along-strike rupture speeds and rupture patterns that are the same as those presented by *Harris and*

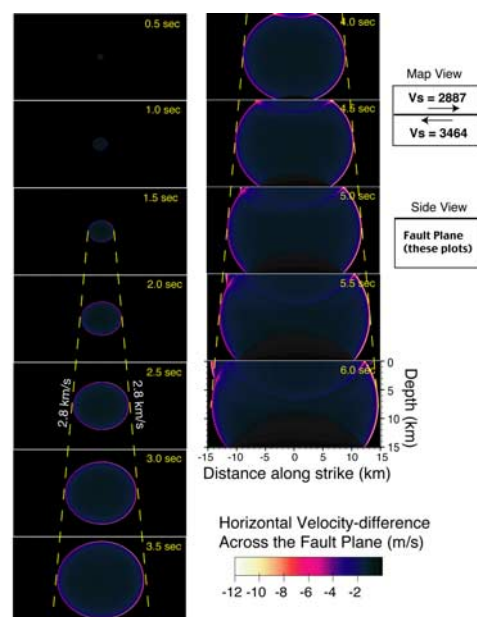


**Figure 3.** (continued)

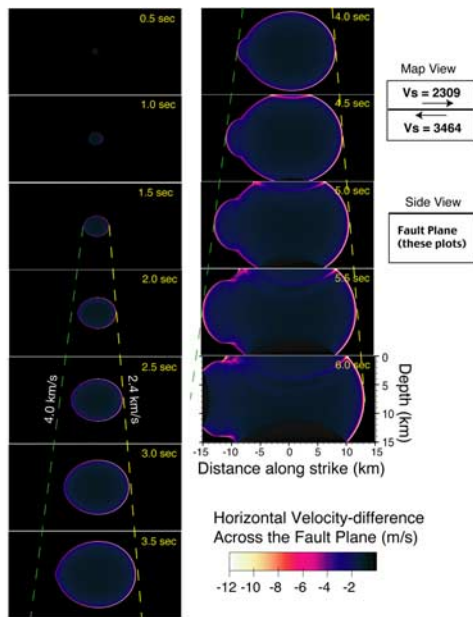


Figure 3. (continued)

Day [1997] for 2D. The 3D case shows along-dip rupture speeds behaving symmetrically, whereby the simulated earthquake propagates at the same speeds up-dip and down-dip, as would be expected from theory for the anti-plane 2D case. In summary, the 3D numerical results support the results from 2D numerical simulations [Harris and Day, 1997], the Parkfield earthquake sequence observations, and laboratory experiments [Xia *et al.*, 2005], all indicating that material contrast is unlikely to induce a preferred rupture direction.

## 6. Discussion and Conclusions

[14] Many earthquakes appear to be predominantly unilateral [McGuire *et al.*, 2002], including Parkfield earthquakes, but this likely is unrelated to material contrast across a fault. Instead, fault geometry [Harris and Day, 1993; Fliss *et al.*, 2005] and stress distribution [Oglesby and Day, 2002; Andrews and Harris, 2005] probably play critical roles in determining rupture extent. McGuire *et al.* [2002] have pointed out that even with a random distribution of nucleation sites, unilateral ruptures will be the rule rather than the exception. While unilateral ruptures are not unusual, material contrasts across faults are unlikely to be their cause. Therefore, further research is needed before reliable prediction of earthquake rupture direction, and thereby the resulting damage, will be possible.

[15] **Acknowledgment.** Thoughtful comments by D. J. Andrews, J. Boatwright, F. Pollitz, D. Oglesby, and an anonymous referee improved the manuscript.

## References

Adams, G. G. (1995), Self-excited oscillations of two elastic half-spaces sliding with a constant coefficient of friction, *J. Appl. Mech.*, *62*, 867–872.

- Andrews, D. J., and Y. Ben-Zion (1997), Wrinkle-like slip pulse on a fault between different materials, *J. Geophys. Res.*, *102*, 553–571.
- Andrews, D. J., and R. A. Harris (2005), The wrinkle-like slip pulse is not important in earthquake dynamics, *Geophys. Res. Lett.*, doi:10.1029/2005GL023996, in press.
- Bakun, W. H., and T. V. McEvelly (1979), Earthquakes near Parkfield, California: Comparing the 1934 and 1966 sequences, *Science*, *205*, 1375–1377.
- Bakun, W. H., and T. V. McEvelly (1984), Recurrence models and Parkfield, California, earthquakes, *J. Geophys. Res.*, *89*, 3051–3058.
- Ben-Zion, Y., and D. J. Andrews (1998), Properties and implications of dynamic rupture along a material interface, *Bull. Seismol. Soc. Am.*, *88*, 1085–1094.
- Boatwright, J., and D. M. Boore (1982), Analysis of the ground accelerations radiated by the 1980 Livermore Valley earthquakes for directivity and dynamic source characteristics, *Bull. Seismol. Soc. Am.*, *72*, 1843–1865.
- Cochard, A., and J. R. Rice (2000), Fault rupture between dissimilar materials: Ill-posedness, regularization, and slip-pulse response, *J. Geophys. Res.*, *105*, 25,891–25,907.
- Day, S. M. (1982), Three-dimensional simulation of spontaneous rupture: The effect of nonuniform prestress, *Bull. Seismol. Soc. Am.*, *72*, 1881–1902.
- Day, S. M., and G. P. Ely (2002), Effect of a shallow weak zone on fault rupture: Numerical simulation of scale-model experiments, *Bull. Seismol. Soc. Am.*, *92*, 3022–3041.
- Dibblee, T. R., Jr. (1971), Geologic map of the Parkfield quadrangle, in *Geologic Maps of Seventeen 15-Minute Quadrangles (1:62,500) Along the San Andreas Fault in the Vicinity of King City, Coalinga, Panoche Valley, and Paso Robles, California, With Index Map*, scale 1:62,500, U.S. Geol. Surv. Open File Rep. 71-87, 17 sheets.
- Eberhart-Phillips, D., and A. J. Michael (1993), Three-dimensional velocity structure, seismicity, and fault structure in the Parkfield region, central CA, *J. Geophys. Res.*, *98*, 15,737–15,758.
- Fletcher, J. B., and P. Spudich (1998), Rupture characteristics of the three M approximately 4.7 (1992–1994) Parkfield earthquakes, *J. Geophys. Res.*, *103*, 835–854.
- Fletcher, J. B., and P. Spudich (2004), Analysis of strong motion at the UPSAR array for the Sept. 28, 2004 M6 Parkfield, CA earthquake, *Eos Trans. AGU*, *85*(47), Fall Meet. Suppl., Abstract S51C-0170M.
- Fliss, S., H. S. Bhat, R. Dmowksa, and J. R. Rice (2005), Fault branching and rupture directivity, *J. Geophys. Res.*, *110*, B06312, doi:10.1029/2004JB003368.
- Gomberg, J. S., P. A. Reasenberg, P. Bodin, and R. A. Harris (2001), Earthquake triggering by seismic waves following the Landers and Hector Mine earthquakes, *Nature*, *411*, 462–466.
- Harris, R. A., and S. M. Day (1993), Dynamics of fault interaction: parallel strike-slip faults, *J. Geophys. Res.*, *98*, 4461–4472.
- Harris, R. A., and S. M. Day (1997), Effects of a low-velocity zone on a dynamic rupture, *Bull. Seismol. Soc. Am.*, *87*, 1267–1280.
- Ida, Y. (1972), Cohesive force across the tip of a longitudinal-shear crack and Griffith's specific surface energy, *J. Geophys. Res.*, *77*, 3796–3805.
- Langbein, J., *et al.* (2005), Preliminary report on the 28 September 2004, M6.0 Parkfield, California earthquake, *Seismol. Res. Lett.*, *76*, 10–26.
- McGuire, J. J., L. Zhao, and T. H. Jordan (2002), Predominance of unilateral rupture for a global catalog of large earthquakes, *Bull. Seismol. Soc. Am.*, *92*, 3309–3317.
- Oglesby, D. D., and S. M. Day (2002), Stochastic fault stress: Implications for fault dynamics and ground motion, *Bull. Seismol. Soc. Am.*, *92*, 3006–3021.
- Ranjith, K., and J. R. Rice (2001), Slip dynamics at an interface between dissimilar materials, *J. Mech. Phys. Solids*, *49*, 341–361.
- Somerville, P. G., N. F. Smith, R. W. Graves, and N. A. Abrahamson (1997), Modification of empirical strong ground motion attenuation relations to include the amplitude and duration effects of rupture directivity, *Seismol. Res. Lett.*, *68*, 199–222.
- Xia, K., A. J. Rosakis, H. Kanamori, and J. R. Rice (2005), Laboratory earthquake along inhomogeneous faults: Directionality and supershear, *Science*, *308*, 681–684, doi:10.1126/science.1108193.

S. M. Day, Department of Geological Sciences, San Diego State University, San Diego, CA 92182, USA. (day@moho.sdsu.edu)

R. A. Harris, U.S. Geological Survey, M.S. 977, 345 Middlefield Road, Menlo Park, CA 94025, USA. (harris@usgs.gov)